Mater.Phys.Mech. 4 (2001) 25-28

NANOSTRUCTURE OF METAL/SEMICONDUCTOR SYSTEM BY SYNCHROTRON X-RAY SCATTERING

C. C. Kim[1], Y. K. Hwu[2], P. Ruterana[3] and J. H. Je[1]

[1] Department of Materials Science and Engineering, Pohang University of Science and Technology, Pohang, Korea
[2] Institute of Physics, Academia Sinica, Nankang, Taipei 11529, Taiwan, Republic of China
[3] Equipe Structure et Comportement Thermomécanique des Matériaux (CRISMAT UMR 6508 CNRS), ISMRA 6, Bd Maréchal Juin, Caen Cedex F-14050, France

Received: July 3, 2001

Abstract. We investigated the nano-structural evolution of metal contacts to GaN during annealing and the correlations between nano-structures and electrical properties for two typical ohmic contacts; Pd as a non-alloyed contact and Ni/Au as an alloyed one. Pd was completely transformed to two kinds of epitaxial Pd gallides, Ga_2Pd_5 and Ga_5Pd, at 700 ºC. In the alloyed Ni/Au contact, the reaction chemistry was rather complicated. Ni_4N formation was found in N_2 annealed sample at 500 ºC of which reaction kinetics was greatly affected by the catalytic effect of Au. The high-temperature compounds were correlated with the rapid degradation of electrical properties during annealing. Meanwhile, the thermal stability of Ni/Au contact greatly improved by suppressing the activated Ni reactivity, which was able to be obtained by forming preferential Ni-O bonding through annealing in air.

1. INTRODUCTION

Nano-structural studies on metal/semiconductor systems are very essential as a functional area of devices keeps reducing, and a high resolved and high fluxed synchrotron x-ray scattering is greatly helpful. In this paper, we present synchrotron x-ray scattering studies on metal contacts to GaN as an example.

The group III nitride semiconductors, especially GaN, are of current interest in view of applications for optoelectronic devices such as light emitting diodes and laser diodes in the blue and violet light region [1, 2]. They are also good candidates for fabricating electronic devices operating at high temperatures due to their superior physical properties, such as the wide bandgap, high breakdown electric field, high saturation velocity, and high thermal conductivity [3, 4]. For reliable, efficient, and high-performance devices, it is essential to develop high quality and thermally stable contacts to GaN-based materials. Extensive studies have been made thus far for developing optimized ohmic contact systems [5, 6].

Pd [7] as a non-alloyed contact and Ni/Au [1, 2] as an alloyed one have been commonly used as an ohmic contact to *p*-type GaN. Many studies on the interfacial reactions between metal and GaN have been carried out in the viewpoint of thermal stability [8-10]. However, the results are still conflicting, and, moreover, important issues such as the nature of the interfacial reactions and the nano-structural phases of metal/*p*-GaN remain unclear. Especially in Ni/Au system, the reaction chemistry is more complicated. Recently, J. K. Ho *et al.* reported a low-resistance ohmic contact to *p*-GaN by oxidizing Ni/Au thin films [11]. The low resistance ohmic contact was primarily attributed to the formation of NiO during oxidation heat treatment. However, thermal stability and nano-structural evolution during the preparation of the contact are not clear either.

In this paper, we present a systematic study on the nano-structural and electrical behavior of the typical ohmic contacts, Pd as a non-alloyed contact and Ni/Au as an alloyed one, on GaN(000l) during annealing. Pd and Ni formed interfacial compounds with GaN at high temperature around 500-700 ºC during annealing in N_2, which is correlated with rapid degradation of electrical properties. In the Ni/Au contact, meanwhile, the thermal stability greatly improved by suppressing the activated Ni

Corresponding author: J.H.Je, e-mail: jhje@postech.ac.kr

© 2001 Advanced Study Center Co. Ltd.

reactivity by means of forming Ni-O bonding through annealing in air.

2. EXPERIMENTAL

The GaN films were grown by metal-organic chemical vapor deposition (MOCVD) on *c*-plane sapphire substrate. An undoped GaN layer with a thickness of 2 μm was grown, followed by the growth of 1.6 μm-thick *p*-type GaN doped with Mg. For deposition of Pd and Ni/Au films, the GaN samples were first cleaned with organic solvents, then etched in $HCl:HNO_3$ (3:1) solution, and finally loaded into an e-beam evaporation system. Thin Pd film of 28 nm thickness was deposited on the cleaned GaN surface. For the Ni/Au film, Ni (10 nm) and Au (12 nm) metals were deposited in sequence.

To examine nano-structural details, the synchrotron x-ray scattering measurements were carried out at beamline 5C2 of Pohang Light Source (PLS) in Korea. The synchrotron x-rays were first focused vertically by a mirror, and a double bounce Si(111) monochromator was used to monochromatize x-rays to the wavelength of 1.488 Å and at the same time to focus the beam in horizontal direction by the saggital focusing second crystal. A four-circle x-ray diffractometer was used to reveal the in-plane crystallinity and the structural orientations of the epitaxially grown overlayers.

3. RESULTS AND DISCUSSIONS

We first examined the as-deposited Pd/GaN interfacial structure using high resolution electron microscope (HREM). The observed cross sectional atomic image was shown in Fig. 1 (a). After digitization of the HREM image, a Fourier transform was calculated and the filtered image was reconstructed [Fig. 1 (b)]. The additional Pd fringes due to the misfit dislocations are visible at the interface. By measuring the atomic spacing between the regularly spaced dislocation cores, we notice that six Ga distances in GaN match to seven Pd distances. The GaN surface etched with aqua regia is atomically clean and the Pd contact to GaN has the interfacial structure, in which six Ga distances (3.189Åx6=19.134Å) in GaN match to seven Pd distances (2.750Åx7=19.250Å), consistent with the x-ray scattering studies previously reported [12]. This interfacial structure enable the large stress caused by the lattice mismatch of 22% to be reduced less than 1%, measured by x-ray scattering [12]. The epitaxial relationships between the as-deposited Pd and GaN films are Pd [111] // GaN [0001] and Pd [1$\bar{1}$0] // GaN [11$\bar{2}$0], as previously reported [13].

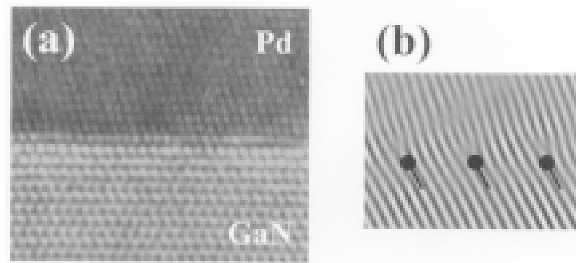

Fig. 1. (a) HREM image of the Pd/sapphire interface region. (b) Fourier filtered image of the Fig. 1 (a), showing misfit dislocations.

As the Pd film was annealed to 700 °C for 30 s in a rapid thermal annealing (RTA) furnace under N_2 flowing atmosphere, the Pd was completely transformed to two kinds of epitaxial Pd gallides by Pd-Ga reaction. Fig. 2 (a) shows the powder diffraction profiles of the post-annealed Pd films on GaN at 700 °C. The Bragg reflections at q_z = 2.772 $Å^{-1}$ and q_z = 2.880 $Å^{-1}$ correspond to the Ga_2Pd_5 (201) (JCPDS 2.762 $Å^{-1}$) and Ga_5Pd (213) (JCPDS 2.878 $Å^{-1}$) reflections, respectively. Both Ga_2Pd_5 and Ga_5Pd phases were grown epitaxially on GaN(0001), which was revealed by the nonspecular Ga_2Pd_5 (221) and the Ga_5Pd (310) reflections that were located 16.1° and 47.2° away from the surface normal direction, respectively. Fig. 2 (b) shows the scattering profile along the phi scans of these nonspecular gallide reflections. The well-defined peaks on the phi scans indicated that the Ga_2Pd_5 and Ga_5Pd phases were in fact grown epitaxially on GaN (0001). From the relative directions of the film and the substrate crystalline axes, we summarized the epitaxial relationships of the two gallides as follows. The Pd-rich gallide, Ga_2Pd_5 has a crystalline orientation with Ga_2Pd_5 (201) // GaN (0001) and Ga_2Pd_5 [010] // GaN [11$\bar{2}$0]. Meanwhile, the Ga-rich gallide, Ga_5Pd has a crystalline orientation with Ga_5Pd (213) // GaN (0001) in the out-of-plane direction, and Ga_5Pd [310] in the same azimuthal angle with GaN [10$\bar{1}$0]. An increased contact resistance during high temperature annealing around 700 °C [14] is attributed to these Pd-Ga compounds.

In an alloyed contact system, Ni/Au is commonly used as *p*-type ohmic contact through annealing in N_2 [15] or air [11]. The reaction chemistry of the alloyed Ni/Au contact is much more complicated. Fig. 3 shows a series of x-ray diffraction profiles for Ni/Au contacts obtained during real-time annealing at 550 °C in N_2 and air. In N_2 annealing, a Ni_4N phase is found as identified by the Ni_4N(111) Bragg reflection. The structural evolution of Ni/Au contact during annealing in N_2 has been studied in our research

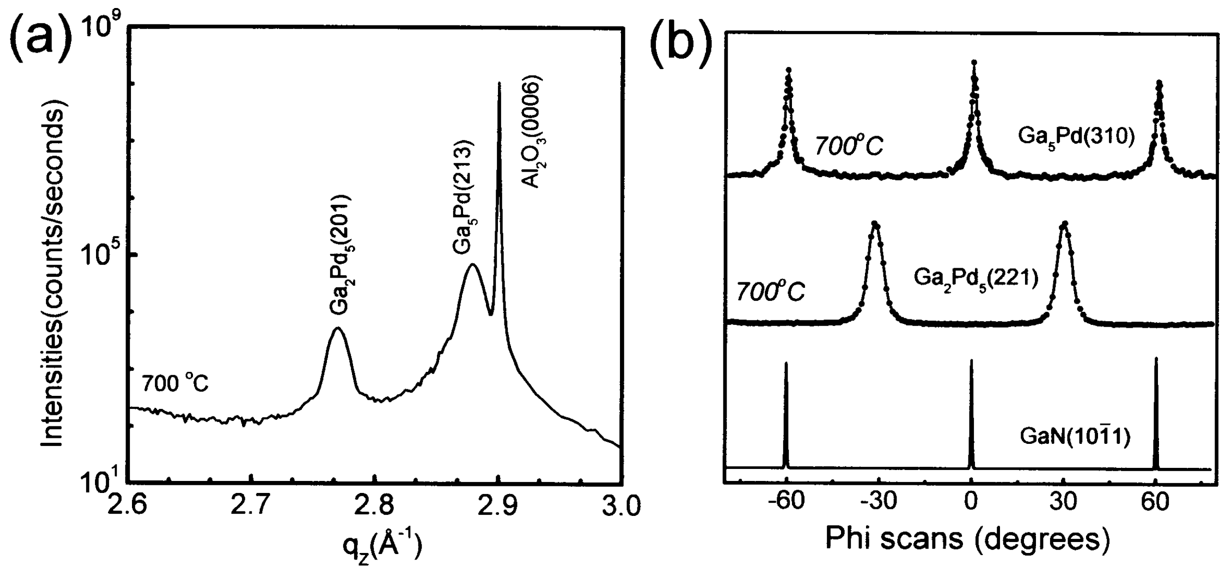

Fig. 2. The x-ray scattering profiles of the 700 °C annealed Pd/GaN films. (a) The powder diffraction pattern along the surface normal q_z direction. (b) The typical phi scans for the GaN (10$\bar{1}$1), Ga_2Pd_5 (221), and Ga_5Pd (310) nonspecular reflections along the azimuthal direction.

group, including GaN decomposition and reactions at 500 °C [16]. We showed that the Ga diffused into Ni and Au substitutional positions, and the decomposed nitrogen reacted with Ni and formed the Ni_4N phase. The kinetics of Ni reaction is activated by Au catalysis [17].

We note that Ni_4N is not detected in air annealing. In fact, almost all of the Ni is in the NiO form at this stage. The NiO signal is, however, hardly seen in Fig. 3 because the weak NiO (111) reflection are under the tails of the GaN(0002) and Au(111) reflection. The large shift of Au (111) reflections is related with alloyed Ni content. The details are reported in [17]. Ni is preferentially bound to strong Ni-O bonding and Ni-N reaction is much limited in the air annealed conditions.

High-temperature compounds formed by reaction with GaN deteriorate electrical properties. The variations of specific contact resistivities of the Ni/Au contacts are displayed as a function of subsequent annealing cycles in Fig. 4. Ohmic contact resistivities were determined using transmission line method (TLM). The TLM test structures were subjected to thermal cycling by rapid thermal annealing under atmospheric pressure of N_2 and air. In each case, the annealing cycle recipe heated the samples to 550 °C and soaked for 1 min. Electrical properties were measured as a function of subsequent thermal cycles. For the N_2 annealed cases, a U-shaped dependence of contact resistivity on the annealing cycles is obtained. However, the air annealed contacts show stabilized contact resistivities. The results indicate the oxidized Ni/Au contacts show better thermal stability than that of N_2 annealed. The origin of deteriorating thermal stability in the N_2 annealing is attributed to Ni_4N formation at the interface between metal and GaN, which becomes severe by the activated Ni reactivity due to Au catalysis.

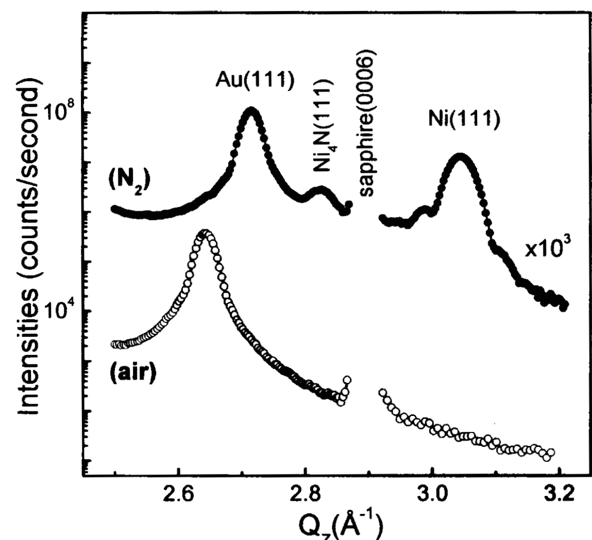

Fig. 3. The x-ray powder diffraction profiles along the surface normal q_z direction for Au/Ni/GaN films measured at 550 °C during real-time annealing in N_2 and air.

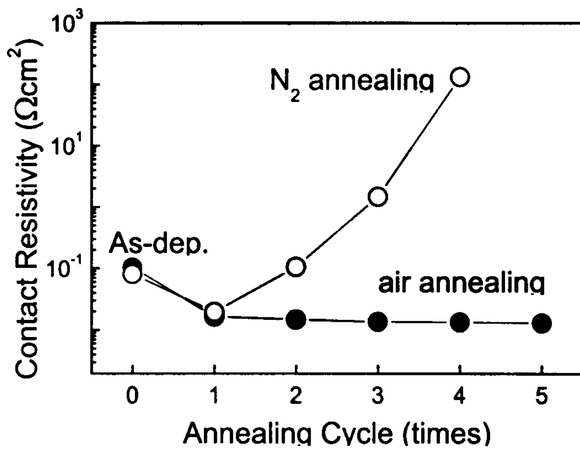

Fig. 4. Variation of contact resistivities as a function of subsequent thermal cycles under atmospheric pressure of N_2 and air.

4. SUMMARY

The high-temperature nano-structural behavior of ohmic metal systems to *p*-type GaN and their resulted electrical properties were studied and reported. We presented two typical ohmic systems, Pd as a non-alloyed contact and Ni/Au as an alloyed one. Pd was completely transformed to two kinds of epitaxial Pd gallides, Ga_2Pd_5 and Ga_5Pd, at 700 °C. In the alloyed Ni/Au contact, Ni_4N formation was found in N_2 annealed sample at 500 °C of which reaction kinetics was greatly affected by the catalytic effect of Au. These compounds were correlated with the rapid degradation of electrical properties at high temperature. Meanwhile, the thermal stability of Ni/Au contact greatly improved by suppressing the activated Ni reactivity, which was able to be obtained by forming preferential Ni-O bonding through annealing in air.

ACKNOWLEDGMENT

This work was supported by the Brain Korea 21 project, by national program of Tera-level Nanodevices, and by Technology Evaluation and Planning (KISTEP) through the NRL project.

REFERENCES

[1] S. Nakamura, M. Senoh and T. Mukai // *Appl. Phys. Lett.* **62** (1993) 2390.

[2] S. Nakamura, M. Senoh, S. Nagahama, N. Iwasa, T. Yamada, T. Matsushita, H. Kiyoku, Y. Sugimoto, T. Kozaki, H. Umemoto, M. Sano and K. Chocho // *Appl. Phys. Lett.* **72** (1998) 2014.

[3] M. A. Khan, M. S. Shur, J. N. Kuznia, Q. Chen, J. Burm and W. Schaff // *Appl. Phys. Lett.* **66** (1995) 1083.

[4] O. Aktas, Z. F. Fan, S. N. Mohammad, A. E. Botchkarev and H. Morkoc // *Appl. Phys. Lett.* **69** (1996) 3872.

[5] Q. Z. Liu and S. S. Lau // *Solid-State Electron.* **42** (1998) 677, and references therein.

[6] S. J. Pearton, J. C. Zolper, R. J. Shul and F. Ren // *J. Appl. Phys.* **86** (1999) 1, and references therein.

[7] J. K. Kim, J. L. Lee, J. W. Lee, H. E. Shin, Y. J. Park and T. Kim // *Appl. Phys. Lett.* **73** (1998) 2953.

[8] J. D. Guo, F. M. Pan, M. S. Feng, R. J. Guo, P. F. Chou and C. Y. Chang // *J. Appl. Phys.* **80** (1996) 1623.

[9] J. K. Sheu, Y. K. Su, G. C. Chi, W. C. Chen, C. Y. Chen, C. N. Huang, J. M. Hong, Y. C. Yu, C. W. Wang and E. K. Lin // *J. Appl. Phys.* **83** (1998) 3172.

[10] H. S. Venugopalan, S. E. Mohney, B. P. Luther, S. D. Wolter and J. M. Redwing // *J. Appl. Phys.* **82** (1997) 650.

[11] J. K. Ho, C. S. Jong, C. C. Chiu, C. N. Huang, C. Y. Chen and K. K. Shih // *Appl. Phys. Lett.* **74** (1999) 1275.

[12] C.C. Kim, W.H. Kim, Jung Ho Je, D.W. Kim, H.K. Baik and S.M. Lee // *Electrochem. Solid-State Lett.* **3** (2000) 335.

[13] U. Tanaka, T. Maruyama and K. Akimoto // *J. Crystal Growth* **202** (1999) 444.

[14] R. Wenzel, G.G. Fischer and R. Schmid-Fetzer // *Mater. Sci. Semicond. Process.* **4** (2001) 357.

[15] J. K. Kim, J. L. Lee, J. W. Lee, Y. J. Park and T. Kim // *J. Vac. Sci. Technol. B* **17** (1999) 2675.

[16] C. C. Kim, J. K. Kim, J. -L. Lam, J. H. Je, M. S. Yi, D. Y. Noh, Y. Hwu and P. Ruterana // *MRS Internet J. Nitride Semicond. Res.* **6** (2000) 4.

[17] C. C. Kim, J. K. Kim, J. -L. Lam, J. H. Je, M. S. Yi, D. Y. Noh, Y. Hwu and P. Ruterana // *Appl. Phys. Lett.* **78** (2001) 3773.